Dosimetry of External Photon Fields Using Unfolding of Scintillation Gamma Spectrometry Data

J. Kluson, Tomas Cechák, Prague

Introduction

The mathematical processing (unfolding) of pulse height spectra from a scintillation detector enables to calculate the photon fluence rate energy distribution in a measured photon field. The data processing is based on the knowledge of the detection system response function [1, 7] (usually approximated by the response matrix) and directional dependence respectively. The other dosimetric quantities - e.g. exposure or air kerma rate, superficial/specific activities of radionuclides, dispersed in the soil surface layer (using the suitable source distribution and experimental arrangement models), etc. - can be calculated from the photon fluence rate.

Main advantages of this approach are: 1) no experimental calibration and corrections of the energy dependence are necessary (both included in the mathematical model and resulting response matrix), 2) high sensitivity (depending on detector volume), 3) spectrometric information, 4) calculation of responses can be provided for any experimental arrangement, including special cases (e.g. accidental contamination of large territory), when experimental calibration is impossible.

Method and applications

The basic principle of designed method is apparent from the flow diagram in Fig. 1.

Full procedure of the detector response matrix calculations is described by second flow diagram in Fig. 2.

The individual experimental arrangements models and Monte Carlo particle transport simulation are used for detector response calculations. Examples of the sets of calculated 3"x3" NaI(Tl) detector response functions for broad parallel beam (incident perpendicularly to the detector endface) and energy intervals up to 3 and 10 MeV are in Fig. 3, 4. The response matrixes with energy bins 15, 30, 60, 90 keV and different energy intervals (according to the application) were prepared from calculated responses. The iterative (Scofield-Gold) method [8, 2] (to solve corresponding matrix equation) is usually used for unfolding of experimental spectra. Using of neural networks for data processing and analysis was also tested.

Developed method of the processing and interpretation of the experimental spectrometric data was used to a wide scope of applications. Dosimetric properties of the method were tested and examples are shown in Fig. 5 (calibration and test of linearity for very low doses region) and Fig. 6 (high sensitivity demonstration for the extremely low background field, both measurements at UDO lab in Asse salt mine).

Next tests of discussed method were performed during the EU intercomparison experiments at Risø and PTB Braunschweig, 1994, where errors of the air kerma rate calculated values were determined. Errors for the free-field calibration experiments (for ^{137}Cs, ^{60}Co, ^{226}Ra and natural background) have not exceeded ±3 % and errors for the high energy calibration (PTB 6 MeV facility) have been in the 5 % band. Figs. 7 and 8 show examples of results of the individual measurements at free field calibration (for ^{226}Ra source) and high energy calibration respectively. The experimental spectrum and calculated air kerma

rate energy distribution respectively are shown on the top and bottom part of the both figures respectively. The spectra codes, mean count rates and total air kerma rates (exposure rates) are marked on the figures.

Example of developed method application in the high energy field is shown on Fig. 9 (field in VVER 440 nuclear power plant reactor hall, 1 meter above centre of the steam generator lid).The older, Ø75 x 75 mm detector and response matrix with wide energy bins (200 keV) were used in this case.

Example of environmental in-situ gamma ray spectrometry result (air kerma rate energy distribution in the usual reference point 1 meter above ground) from partly restored depository of wastes from uranium ore pre-processing is shown in the Fig. 10.

Method was applied for monitoring of the gamma fields in the spent fuel temporary storage and study of its influence on the radiation fields in the storage close neighbourhood. Measured differential air kerma rate distributions in one of the selected reference points near to storage building are shown in the Figs. 11 and 12. First measurement was done for empty storage, second after storing first 6 containers (Castor type). Comparison of those results gives the first evidence of negligible impact of the storage on radiation in neighbourhood.

Conclusions

Described method was successfully used for environmental gamma ray fields study, monitoring and analysis, natural background components and variations studies [6], study of environmental impact of uranium ore mining and processing, assessment of doses in dwellings, workplaces monitoring (including mentioned nuclear power plant and spent fuel temporary storage), processing of the environmental spectral data from Chernobyl region, works within the project of Semipalatinsk nuclear weapon test site radiological assessment [3], etc.

Calibration factors for determination of the superficial/specific activities from scintillation or semiconductor detectors spectrometry data were calculated (for defined experimental arrangements). Calculations were done for natural radionuclides (^{40}K and U, Th - series) as well as for ^{137}Cs and set of another expected significant man-made contaminants.

The calibration (response functions calculations) and data processing method for airborne gamma ray scintillation spectrometry (system ENMOS, produced by PICODAS Group. Inc., Canada) were developed on the similar basis [4]. Method was successfully introduced and can be used for fast and effective operational or accidental radioactive contamination monitoring/mapping over the large areas [5]. Method makes it possible to calculate concentrations of the natural radionuclides and man-made contaminants (with given depth distributions models) from airborne spectrometry data. The individual scans (i.e. usually 1 s experimental spectra), measured over the monitored area, are processed and corresponding maps of individual radionuclides dispersions can be constructed. The exposure (or air kerma) rate distribution over the same area can be calculated from determined individual radionuclides concentrations.

References

1. Berger, M.J., Seltzer, S.M.: Response Functions for Sodium Iodine Scintillation Detectors. NIM 104 (1972) 317-332.

2. Clements, P.J.: A Discussion of Variations on the Scofield-Gold Iterative Deconvolution Technique. AERE - R 7222 (1972).

3. Hill, P., Hille, R., Bouisset, P., Calmet, D., Kluson, J., Smogulov, S., Seysebaev, A.: Radiological Assessment of Long Term Effects at the Semipalatinsk Testsite. NATO-Semipalatinsk Project 1995/1996, Berichte des Forschungs-

zentrums Jülich, JÜL - 3325 December 1996, ISSN 0366-0885.
4. Kluson, J.: Calculation of the Field Spectrometer Response and Calibration for the Operational and Accidental Monitoring of Nuclear Power Plant Neighbourhood. Progress in Nucl. Energy 24 (1990) 377-383.
5. Kluson, J., Malušek, A., Cechák, T., Jurza, P.: Airborne Gamma-Ray Spectrometry in Environmental and Accidental Monitoring. In Proceedings of IRPA9 International Congress on Radiation Protection, April 14-19 1996, Vienna, Austria.
6. Pernicka, F., Kluson, J.: Variations of Natural Radiation Background and their Effect on Detector Response. Environ. Internat. 22, Suppl. 1 (1996) 85-91.
7. Rogers, D.W.O.: More Realistic Monte Carlo Calculations of Photon Detector Response Functions. NIM 199 (1982) 531-548.
8. Scofield, N.E.: Iterative Unfolding. NAS - NS - 3107 (1963) 108.

Figure 1: Flow diagram of the method for the full data processing and analysis

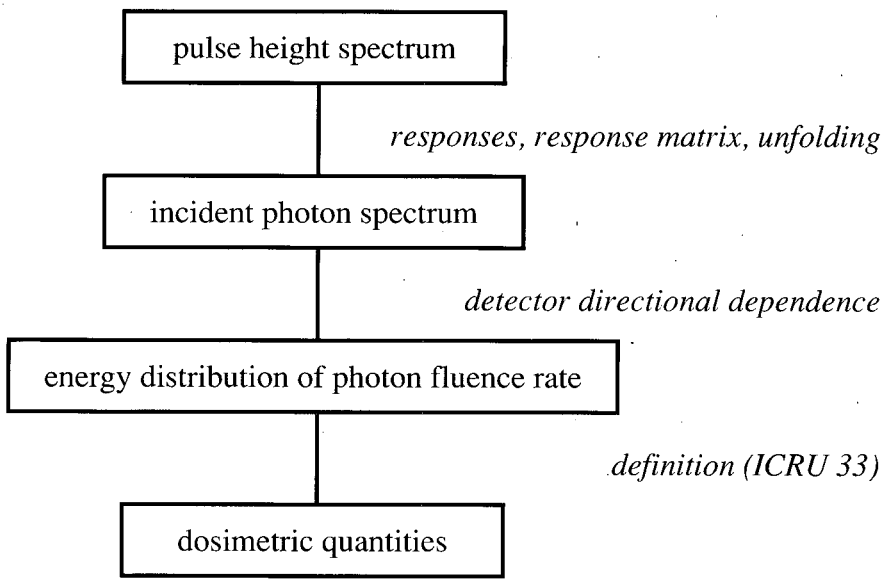

Figure 2: Calculation of the detector response and response matrix - flow diagram

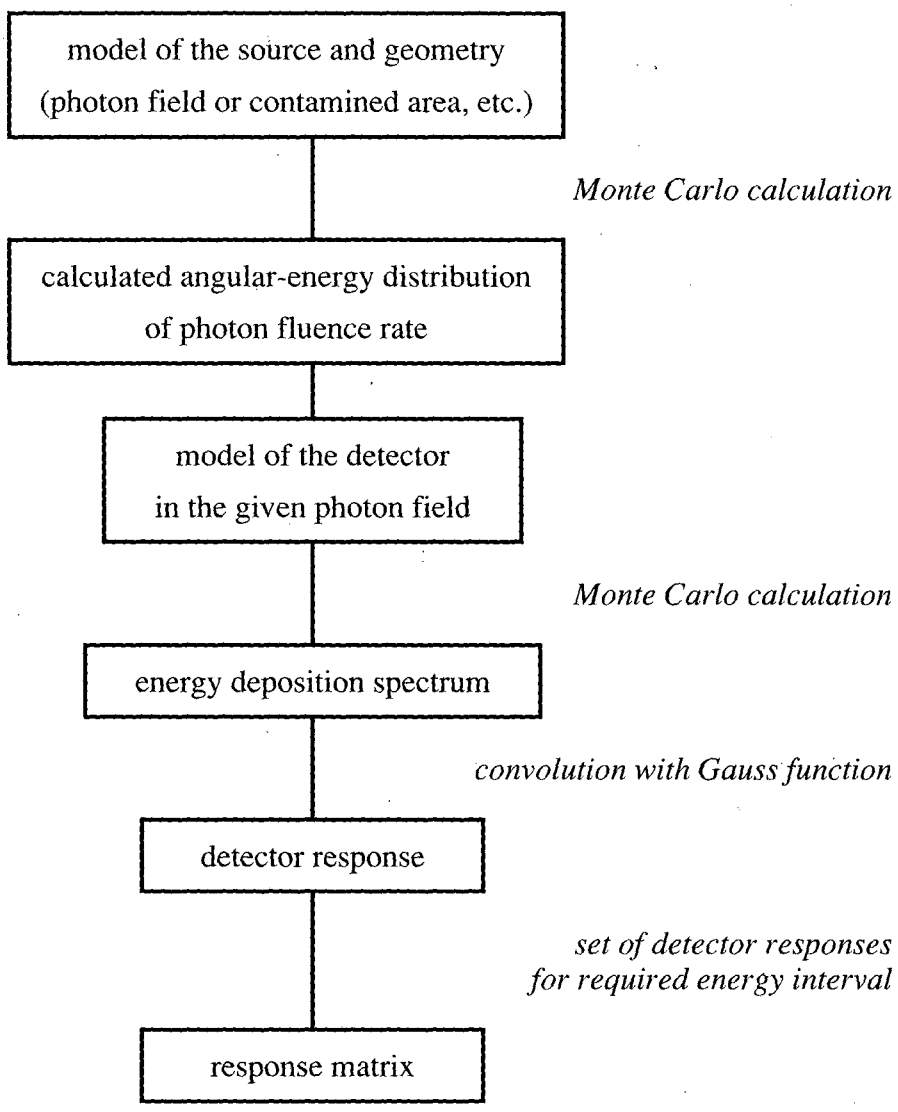

Figure 3

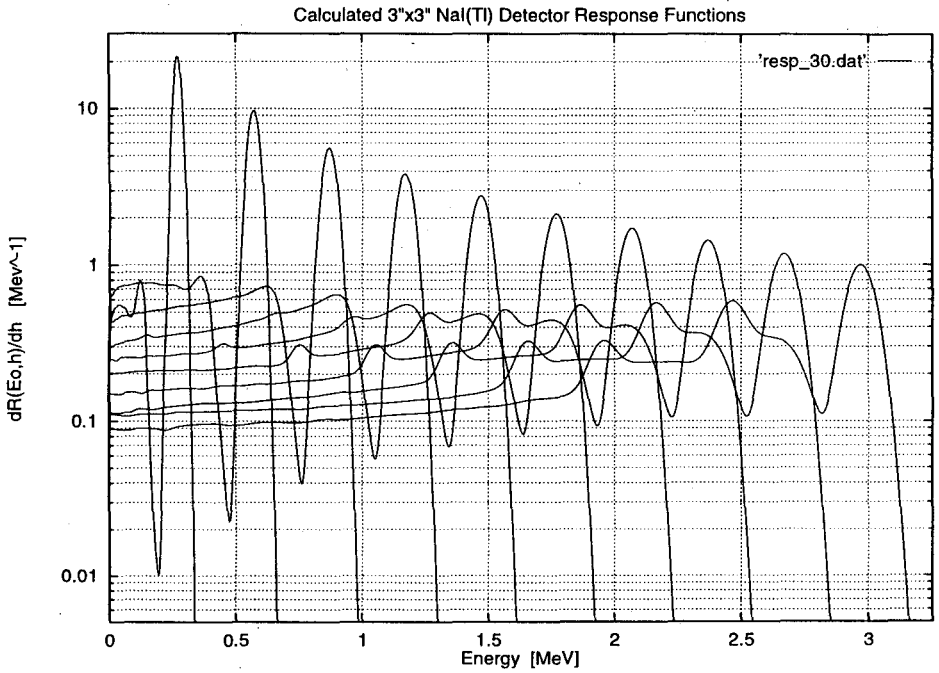

Figure 4

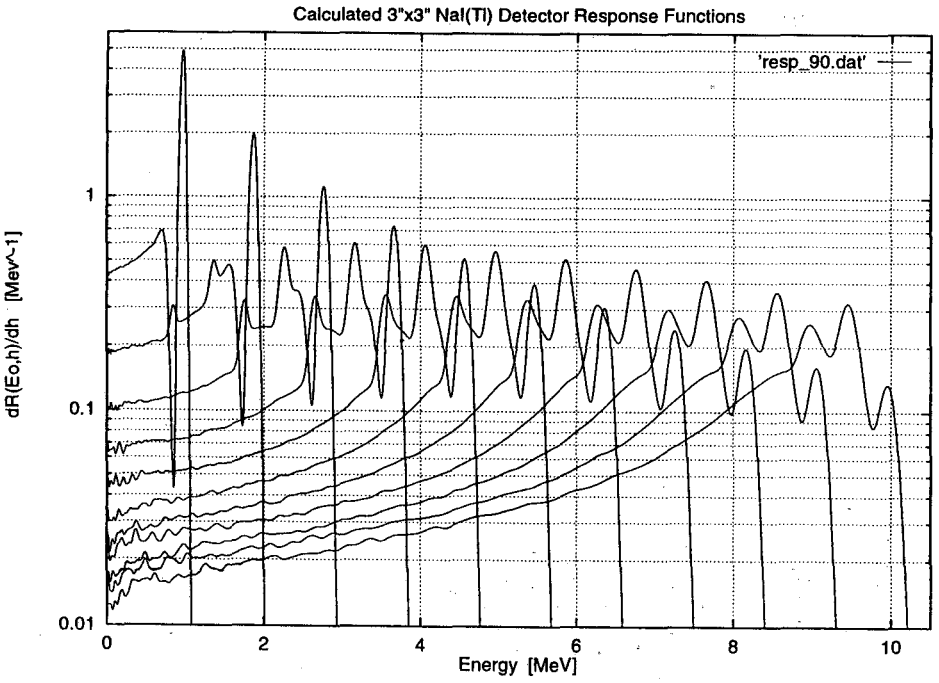

Figure 5: **UDO lab in the Asse salt mine, test of linearity for low doses**

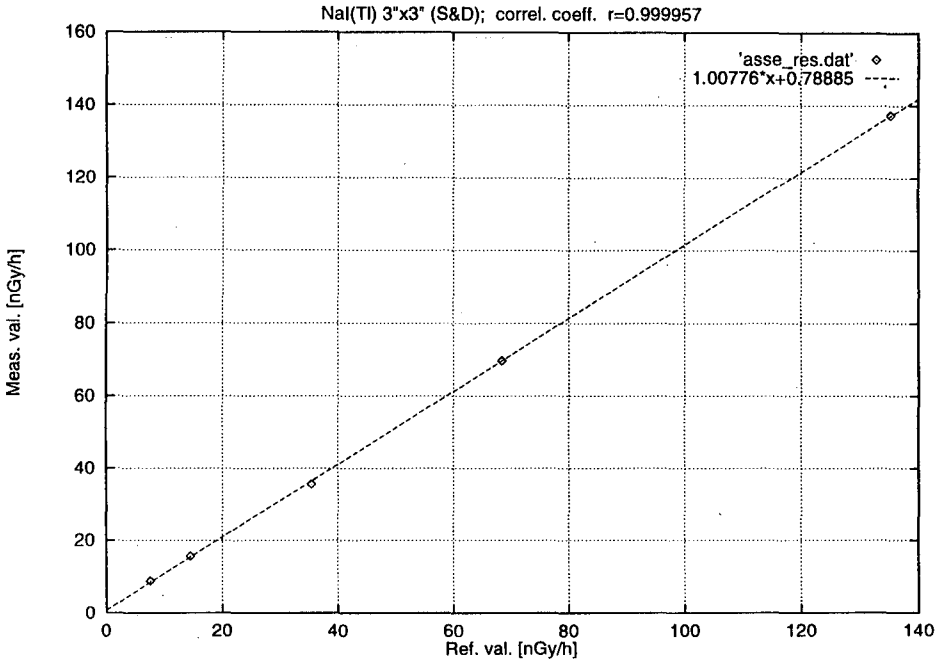

Figure 6: **UDO lab in the Asse salt mine, background with shield**

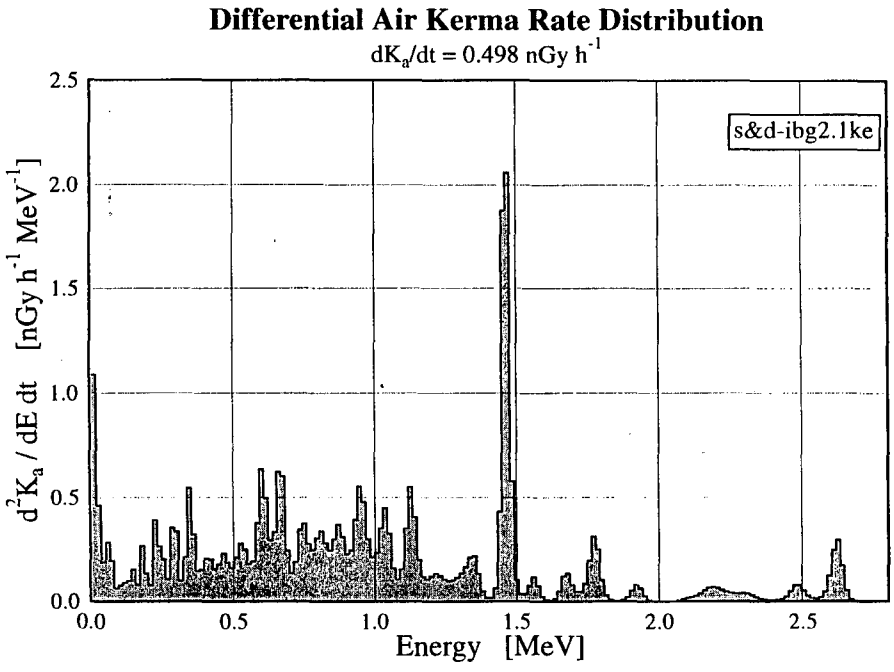

Figure 7: **Free field calibration, ^{226}Ra source, distance 10 metres**

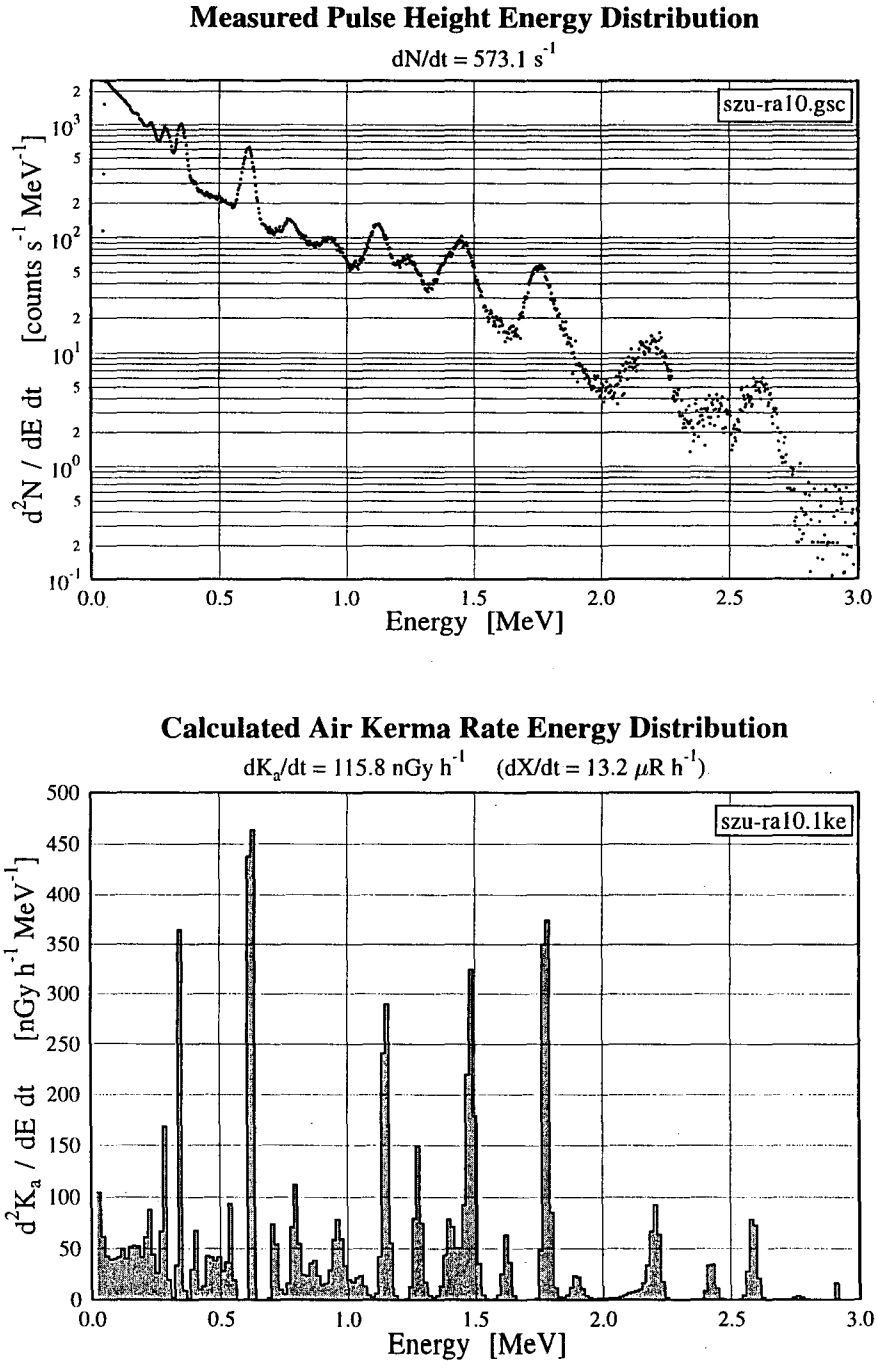

Figure 8: **PTB - 6 MeV facility, calibration measurement, distance 3 meters from the target**

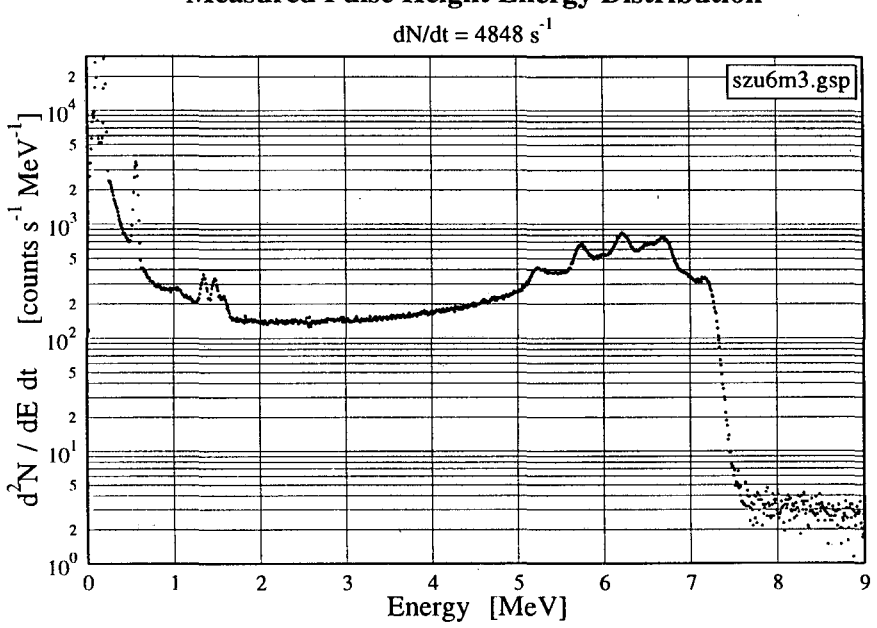

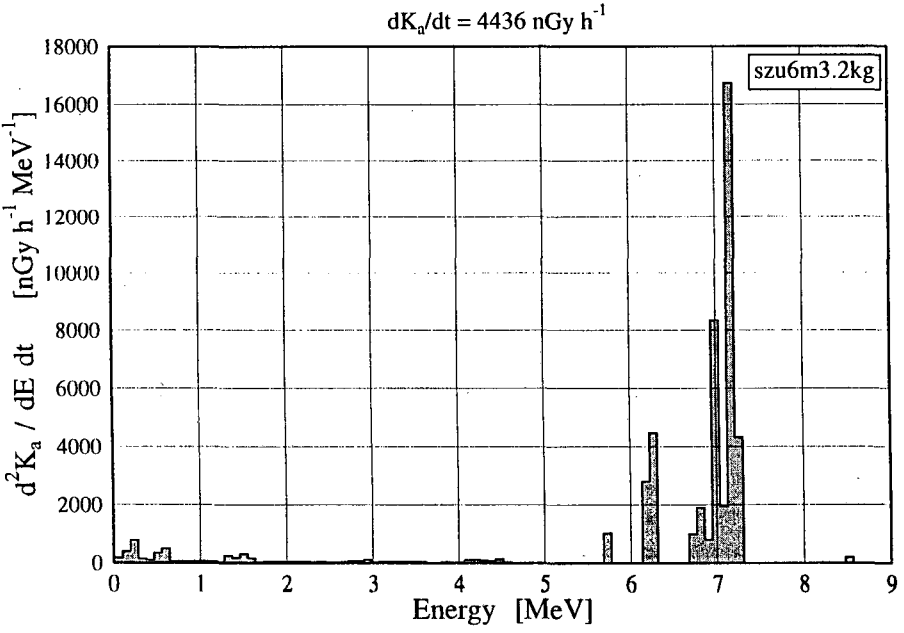

Figure 9: **VVER 440 nuclear power plant reactor hall, steam generator lid**

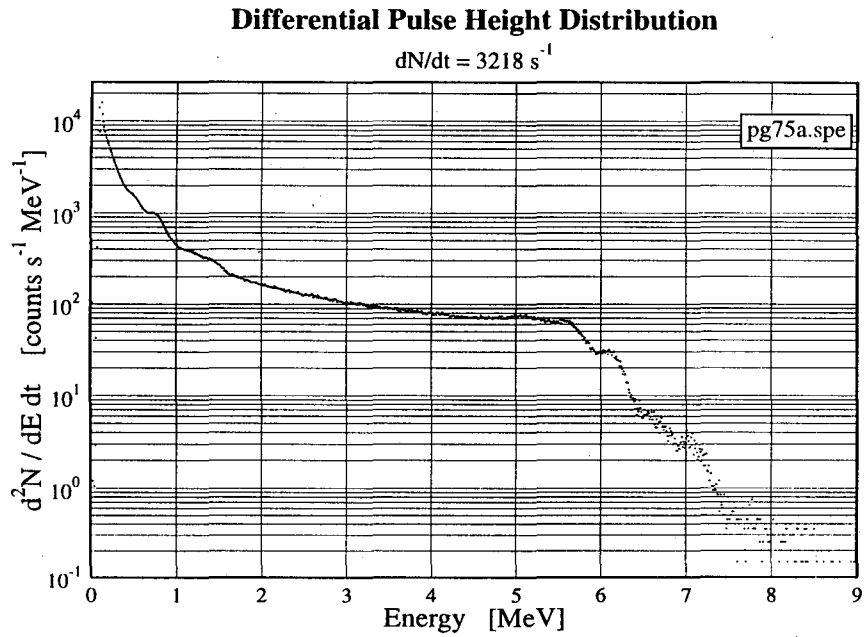

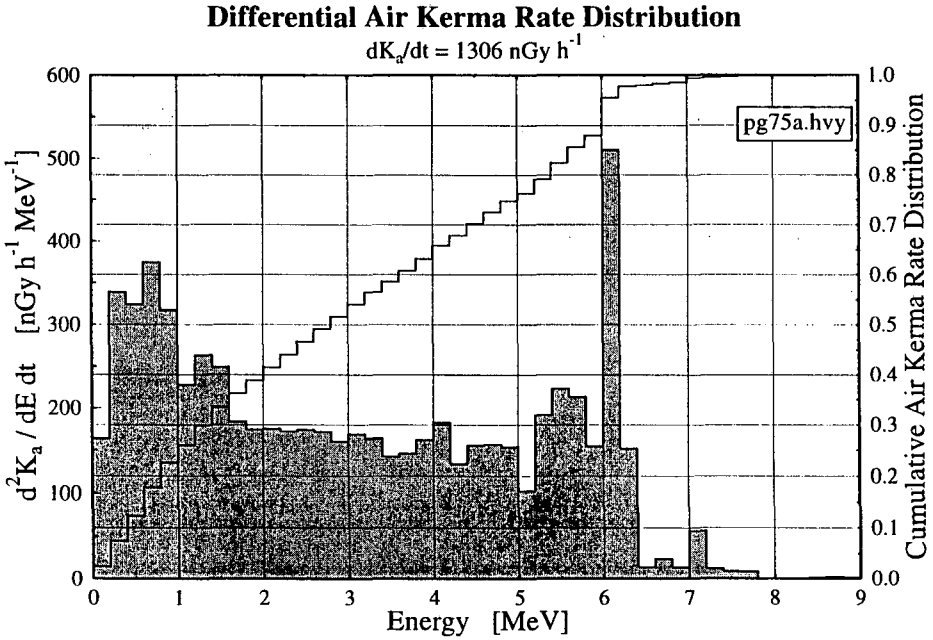

Figure 10: **Depository of wastes from uranium ore pre-processing, 1 meter above ground**

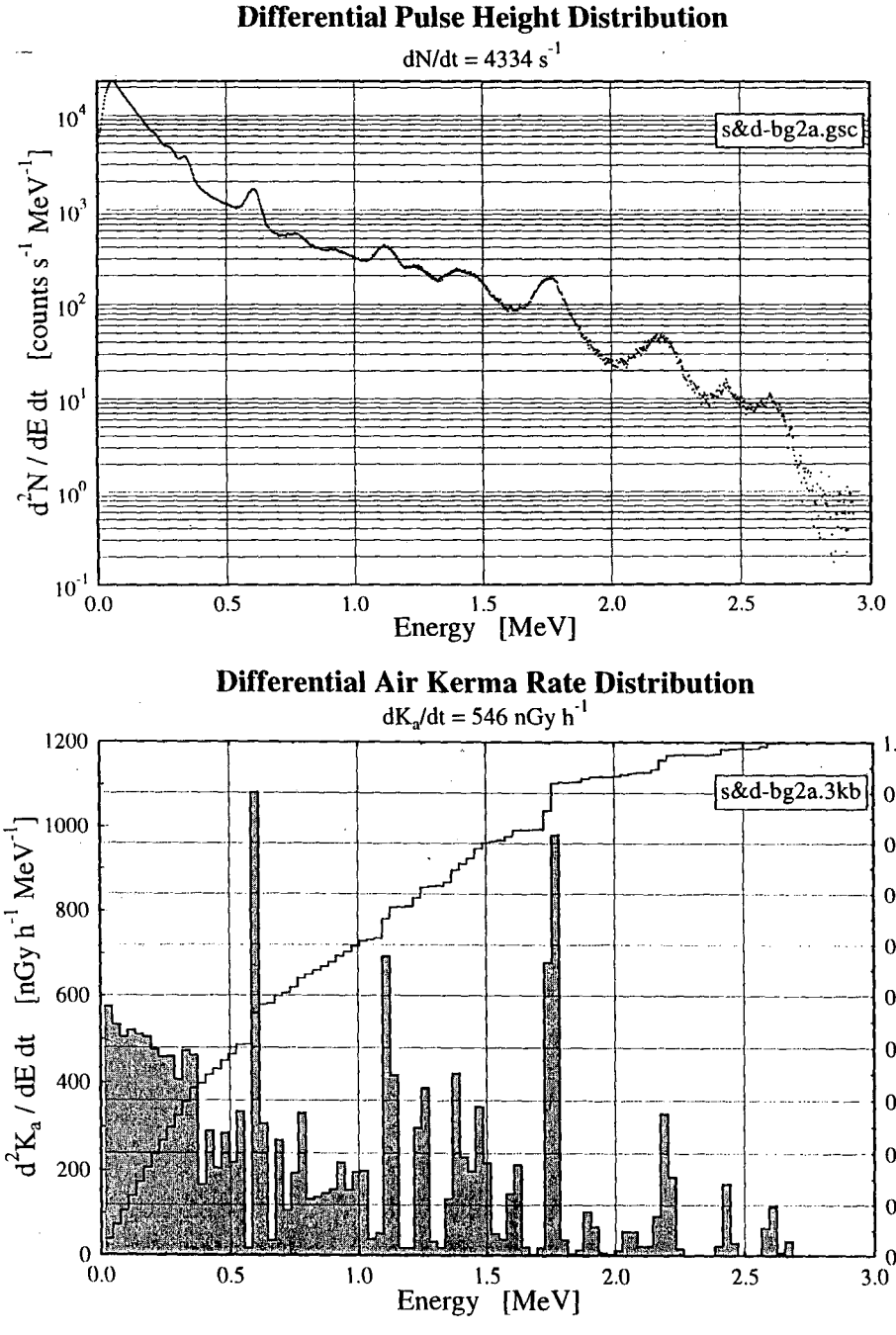

Figure 11: **Background in reference point near to spent fuel temporary storage (empty storage)**

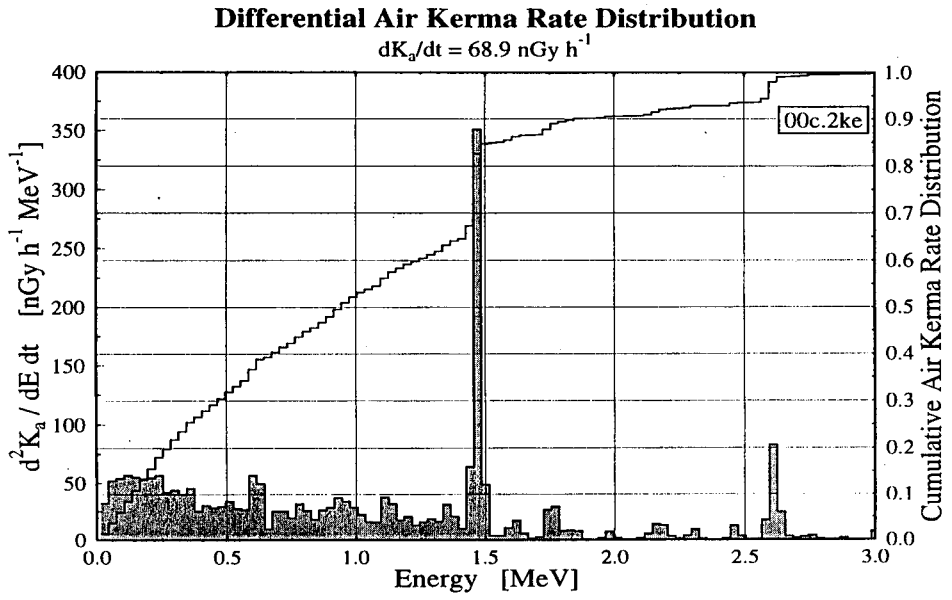

Figure 12: **Background in reference point near to spent fuel temporary storage (with 6 Castor containers)**